ACS OMEGA

Open Access

http://pubs.acs.org/journal/acsodf

Article

A Chimeric LBT-GFP Biosensor Exhibits Antithetical Fluorescence Responses to Ca^{2+} and Dy^{3+} Binding

Jingyao Li,[§] Sandra Oloketuyi,[§] Li-Wei Hung, Nilusha Sudasinghe, Sang-Min Shin, and Ramesh K. Jha*

Cite This: *ACS Omega* 2026, 11, 20235−20240

Read Online

ACCESS | Metrics & More | Article Recommendations | Supporting Information

ABSTRACT: Rare earth elements (REEs) are critical components in emerging technologies, but their mining and refining processes are often laborious, costly, and environmentally damaging. Developing green and efficient separation methods for REEs is crucial. Biomolecular approaches using lanthanide-binding proteins and peptides show promise for selective REE extraction and separation. In this study, we present the design and characterization of a genetically encoded fluorescence indicator (GEFI) construct that combines a superfolder green fluorescent protein (sfGFP) with a dual lanthanide-binding tag (2×dLBT). The 2×dLBT insert induces conformational changes in sfGFP upon lanthanide binding, modulating the fluorescence intensity. The sfGFP-2×dLBT biosensor exhibited distinct fluorescence responses to different lanthanide ions, with the highest dynamic range observed for heavy REEs like dysprosium (Dy^{3+}). Interestingly, the sensor displayed an antithetical response, where low concentrations of lanthanides initially quenched the fluorescence, but higher concentrations led to a significant fluorescence increase (1.5-fold). The Ca^{2+} ion on the other hand showed only a dose-dependent quenching of the fluorescence response. Based on these observations, the biphasic response of the biosensor to lanthanides was eliminated by pretreating the sensor with calcium, which further expanded the dynamic range up to 3-fold for Dy^{3+}. The lanthanide-selective and concentration-dependent fluorescence changes of the sfGFP-2×dLBT biosensor demonstrate its potential as a platform for developing specific sensors for various REEs. These sensors could enable rapid and cost-effective determination of REE composition in complex mixtures, facilitating the separation and recovery of critical REEs from electronic waste and other REE-containing sources.

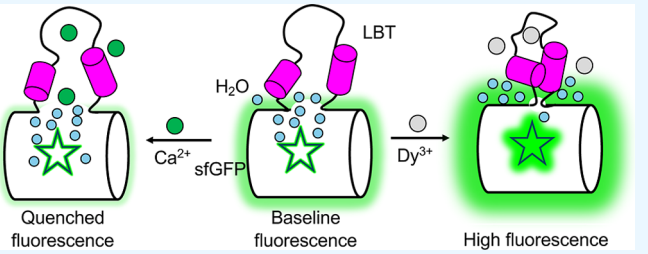

INTRODUCTION

Rare earth elements (REEs) that mainly constitute f-block elements such as lanthanides are essential components in emerging technologies for defense, renewables, medical applications, and electronics.[1,2] However, lanthanide mining and refinery operations have proven not only laborious and costly due to the chemical similarities of lanthanide ions (Ln^{3+}) but also highly damaging to the local environment as they generate a significant amount of hazardous waste.[3,4] Therefore, new approaches are necessary for the "green" and efficient separation of lanthanides.

Solid-state extraction using biomolecules and biological ligands shows great potential for environmentally sustainable lanthanide separation process development. The discovery and engineering of lanthanide binding proteins and peptides such as Lanthanide-Binding Tags (LBTs) and Lanmodulin (LanM) have enabled the bioengineering of a lanthanide-specific bioadsorbent with high binding affinity and selectivity toward lanthanides over other metal ions.[5−7] Recent studies have applied them in the reversible separation of lanthanide from nonlanthanide metals.[8,9] However, the selective separation of individual lanthanides remains challenging, despite its importance for element-specific applications.

In this study, we present a genetically encoded fluorescence indicator (GEFI) construct that combines superfolder green fluorescent protein (sfGFP)[10] with lanthanide-binding tags (LBTs).[11] Engineered GFPs have been used as reporters for proteins that undergo conformational changes upon ligand binding.[12,13] In our design, the LBT serves as the Ln^{3+} binding domain and is inserted near the chromophore of the sfGFP to induce conformational changes upon Ln^{3+} binding, which modulate solvent access to the chromophore and consequently affect the fluorescence (Figure 1). Furthermore, the engineered sfGFP-2×dLBT biosensor exhibited distinct responses to different Ln^{3+} ions, offering a potential platform for developing REE-specific binding peptides.

Received: September 29, 2025
Revised: February 27, 2026
Accepted: March 10, 2026
Published: March 24, 2026

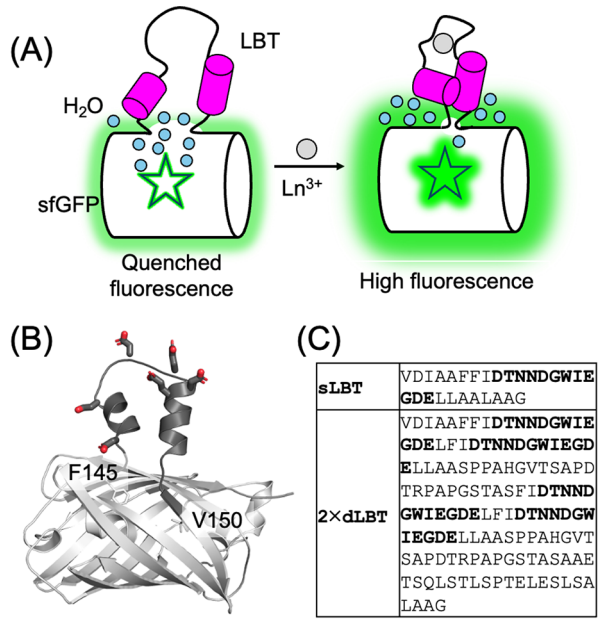

Figure 1. Genetically encoded fluorescence indicator. (A) A cartoon of sfGFP/LBT chimera perturbing the chromophore (shown as a star) environment. (B) AlphaFold2 model of the chimera, sfGFP (light gray) with labeled native F145 and V150 between which the LBT was inserted; single LBT (dark gray) with negative charged amino acids (aspartate and glutamate) that would coordinate with trivalent cations are shown in sticks. (C) Amino acid sequence of LBTs. The repeating metal coordinating segment is shown in bold. sLBT: single lanthanide-binding tag, 2×dLBT: 2-fold double lanthanide-binding tag.

RESULTS AND DISCUSSION

Green fluorescent protein (GFP) molecules have been used as the scaffold of biosensors for multiple target molecules including PFAS and metal ions.[12,13] A binding domain is inserted into the GFP, which undergoes a conformational change upon binding to the target molecule and consequently alters the fluorescence intensity. Biosensor LanTERN showed comparable binding and fluorescence response to light REEs such as La^{3+} and Nd^{3+} and heavy REEs such as Dy^{3+} and Tb^{3+}.[14] Furthermore, the detection module in LanTERN consists of a calmodulin binding peptide (CBP) in the N-terminus and Ca^{2+} binding calmodulin (CaM) in the C-terminus with key residues from a lanthanide binding protein, LanM,[7] transferred to CaM for altering the specificity broadly to Ln^{3+}. To reduce the dependency on the two fragmented modules of CaM/CBP, we chose lanthanide-binding tags (LBTs), which have been reported to exhibit high specificity for different REEs. LBTs exhibit approximately 50-fold higher dissociation constants (K_d) for light REEs (e.g., La^{3+}) than for heavy REEs (e.g., Dy^{3+}), indicating weaker binding affinity to light REEs.[15] This approach has an advantage over the CaM/CBP format as it circumvents the potential disruption of CaM/CBP interaction critical for fluorescence gain during any envisioned mutagenic study for generating specificity in biosensors for each REE.

We first created a chimeric GEFI protein, sfGFP-sLBT, by inserting a single LBT (sLBT) peptide on strand 7 (between residues 145−150) of the sfGFP protein, a site very close to the GFP chromophore, such that lanthanide binding perturbs the solvated environment of the chromophore, affecting the fluorescence response (Figure 1A, Table S1). Figure 1B shows a structure of sfGFP-sLBT predicted by AlphaFold2.[16] However, upon addition of lanthanides (La^{3+}, Nd^{3+}), we did not see any fluorescence increase (Figure S1), though minor quenching effects were observed especially for Nd^{3+} at increasing concentrations. Divalent calcium ions (Ca^{2+}) were also tested and showed no appreciable change in fluorescence above the baseline. These results indicated that lanthanide binding did not trigger an appreciable conformational change on the sLBT that would be needed for a significant change in the solvent accessibility of the GFP chromophore.

With the unpropitious results from sfGFP-sLBT, we hypothesized that a longer lanthanide-binding insert could help perturb the fluorophore environment further, which will allow a larger dynamic range of the biosensor. Therefore, we replaced the sLBT with a much larger 2×dLBT module (Figure 1C, Table S1), consisting of four Ln^{3+} binding sites and inserted at the same site on strand 7 (between residues 145−150) of the sfGFP. A similar 2×dLBT domain had proved to be efficient for lanthanide sequestering when displayed on the cell surface.[9] The AlphaFold2 structure predictions indicated that 2×dLBT is highly unstructured (Figure S2), indicating the possibility of further exposing the sfGFP fluorophore with this inset in a metal-free state. Since 2×dLBT has four Ln^{3+} binding sites, the conformational changes induced upon Ln^{3+} binding would be more dramatic, causing a substantial change in the chromophore environment affecting the fluorescence intensity in the biosensor. To validate our hypothesis, we tested the sfGFP-2×dLBT response to various lanthanides, including La^{3+}, Nd^{3+}, and Dy^{3+}, which exhibit different ionic radii (La^{3+} > Nd^{3+} > Dy^{3+}). Compared to the sLBT insertion, 2×dLBT showed approx-

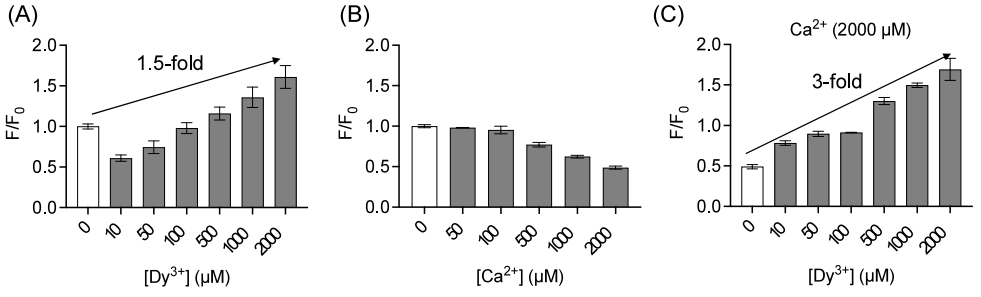

Figure 2. The antithetical effects of alkaline earth and lanthanide on the sfGFP-2×dLBT biosensor at 0.5 μM protein concentration. (A) Dose−response of Dy^{3+} that shows fluorescence quenching at low concentrations but an increase in fluorescence response at higher metal concentrations. (B) Dose−response of Ca^{2+} that shows fluorescence quenching. (C) Dose−response of Dy^{3+} in the presence of 2 mM Ca^{2+}. F_0 is the baseline fluorescence signal of sfGFP-2×dLBT in the absence of any metal.

https://doi.org/10.1021/acsomega.5c10135
ACS Omega 2026, 11, 20235−20240

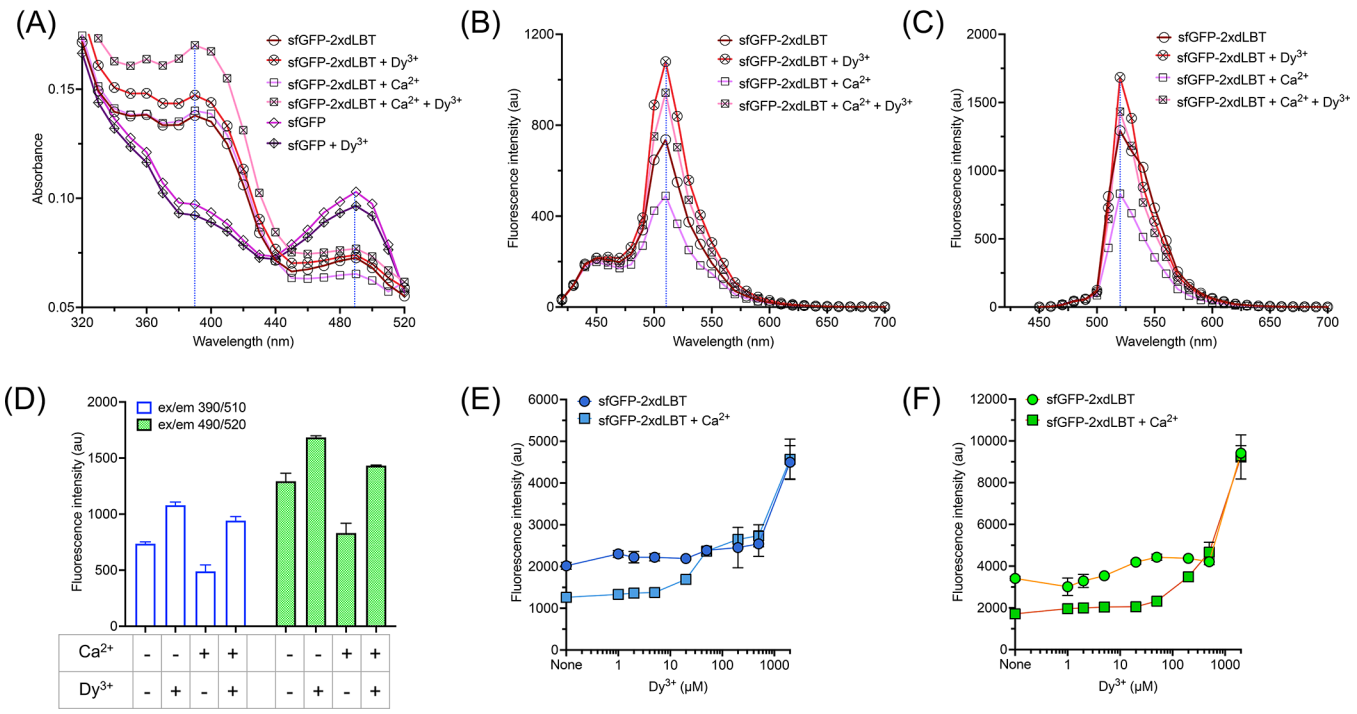

Figure 3. Spectroscopic characterization of lanthanide-bound and unbound sfGFP-2×dLBT. (A) UV−visible (320−520 nm) absorption spectra of the chimeric protein in the absence and presence of Dy^{3+}. The characteristic sfGFP absorption bands are shown for reference. Two absorption maxima at 390 and 490 nm are indicated by dotted lines. Full UV−vis (300−700 nm) spectra are available in the Supporting Information. (B) Emission spectra of sfGFP-2×dLBT upon excitation at 390 nm, showing a fluorescence maximum at 510 nm (dotted line). (C) Emission spectra upon excitation at 490 nm, exhibiting a maximum at 520 nm (dotted line). (D) Fluorescence response of the biosensor (10 μM) in the presence of 4-fold molar excess Dy^{3+} and/or 2 mM Ca^{2+}, measured at excitation/emission pairs of 390/510 nm and 490/520 nm. (E) Lanthanide dose−response curve for sfGFP-2×dLBT (5 μM) monitored at 390/510 nm in the absence and presence of 2 mM Ca^{2+}. (F) Lanthanide dose−response curve monitored at 490/520 nm in the absence and presence of 2 mM Ca^{2+}. All experiments were performed with n = 3 independent replicates. Data are presented as mean ± standard deviation. Error bars are omitted from spectral scans for visual clarity.

imately 5-fold lower fluorescence intensity under metal-free conditions, possibly due to the quenching effect induced by higher structural perturbation and solvation of the chromophore of the chimeric protein sfGFP-2×dLBT. While we observed different dynamic range of responses for these trivalent ions (highest in Dy^{3+} and lowest in Nd^{3+}) (Figure S3), the dose−response of sfGFP-2×dLBT appeared to be two-phased: a drop in fluorescence from the baseline at a low concentration of lanthanide (such as 10 μM) and then a dose-dependent increase in the fluorescence intensity with increasing lanthanide concentration. For example, Dy^{3+} showed a 50% drop at 10 μM but an ∼50% increase at 2000 μM over its baseline fluorescence intensity (Figure 2A). The higher response for Dy^{3+} than that for La^{3+} is consistent with LBT showing stronger binding affinities to heavier REE ions over light REEs.[15]

To determine the specificity of the sfGFP-2×dLBT design, we tested the fluorescence response of sfGFP-2×dLBT to calcium ions. Compared to the buffer control, a decreasing trend in the fluorescence intensity of the sfGFP-2×dLBT sensor was observed with the dosage of calcium ions. The signal dropped by ∼60% at 2 mM concentration of Ca^{2+} (Figure 2B). Other alkaline earth metals or transition metals such as Mn^{2+}, Mg^{2+}, Zn^{2+}, and Ni^{2+} did not show any significant difference in fluorescence intensity at 2 mM concentration. A few divalent and trivalent metals such as Cu^{2+}, Al^{3+}, and Fe^{2+} (susceptible to oxidation to Fe^{3+}) showed quenched fluorescence in the chimeric biosensor (Figure S4), which could also be as a result of an induced precipitation/aggregation, post addition of metal.

We hypothesized that the conformational changes of sfGFP-2×dLBT upon metal ion binding would first lead to an increased opening of the chromophore to the aqueous environment, quenching its fluorescence further compared with that of the apo-state. With the increase of metal ion concentration such as Ln^{3+}, 2×dLBT becomes more structured and consequently reduces solvent access to the chromophore. As a result, the fluorescence signal elevated significantly when the Ln^{3+} concentration was further increased from the concentration that showed the initial decline. While 2×dLBT showed negligible binding affinity to most other metal ions, it is known to bind the calcium ion with a weaker affinity than to any lanthanides.[5] Therefore, Ca^{2+} was able to trigger the first stage of conformational changes and quench the biosensor. However, the fluorescence would not revert in the case of calcium because of its relatively low binding affinity to 2×dLBT, which prevented the stabilization of the conformation even when its concentration was further increased.

While the sfGFP-2×dLBT biosensor exhibited dose-dependent, lanthanide-selective fluorescence responses, the signal was nonlinear to lanthanide concentration, and the dynamic range was still relatively low compared with the buffer control (∼50% increase in fluorescence for Dy^{3+}). In order to see if we could introduce an antithetical response to improve the dynamic range of the biosensor, we included 2 mM calcium in the HEPES buffer to bring the initial fluorescence signal of the

https://doi.org/10.1021/acsomega.5c10135
ACS Omega 2026, 11, 20235−20240

biosensor down by quenching the chromophore with Ca^{2+} binding. With the addition of lanthanides, Ca^{2+} is expected to be outcompeted by any other lanthanide due to its relatively lower binding affinity. Our results showed that the dynamic range expanded dramatically with the pretreatment of calcium from a 50% increase to an over 200% increase (3-fold change) with the dosage of Dy^{3+} (Figure 2C). While La^{3+} sensing did not show an appreciable gain in response upon fluorescence quenching using calcium ions, Nd^{3+} showed a dose-dependent fluorescence increase by 150% in the sfGFP-2×dLBT biosensor (Figure S5).

Overall, we observed a correlation between the biosensor response and the intrinsic binding affinity of each lanthanide to the LBT motif. As reported by Nitz et al.,[15] LBT binding affinity scales with ionic radius, with Dy^{3+} and Tb^{3+} exhibiting the highest affinities and La^{3+} the lowest. This relationship is reflected in the ionic radius trend ($Tb^{3+} \approx Dy^{3+} < Nd^{3+} < La^{3+}$) and the corresponding affinity trend ($Tb^{3+} \approx Dy^{3+} > Nd^{3+} \gg La^{3+}$).[15] Consistent with these properties, our sfGFP-2×dLBT biosensor shows the strongest fluorescence enhancement with Dy^{3+} (Figure 2C) and Tb^{3+} (Figure S4B), followed by Nd^{3+} and La^{3+} (Figure S5).

Encouraged by these observations, we next examined whether chimeric sfGFP-2×dLBT retained the excitation and emission properties of sfGFP or whether these features were altered. We reasoned that identifying the most accurate excitation/emission wavelengths would improve the biosensor's sensitivity and dynamic range. Spectroscopic analysis of purified sfGFP-2×dLBT (10 μM) revealed the appearance of a new absorbance peak at 390 nm in addition to the expected ∼490 nm peak (Figure 3A). No other absorption maxima were detected within the 300−700 nm UV−vis range (Figure S6). The absorbance of sfGFP-2×dLBT increased upon the addition of lanthanide ions (40 μM Dy^{3+}), with an even more pronounced increase when Ca^{2+} (2 mM) was present along with lanthanide. As controls, UV−vis scans of sfGFP and FR-GFP (folding reporter)[10] showed only the characteristic ∼490 nm peak (Figure S7). Upon addition of Dy^{3+}, FR-GFP exhibited an increase in absorbance, along with a blue shift to ∼480 nm. Both GFP variants displayed similar emission spectra, although sfGFP showed a higher fluorescence intensity than FR-GFP, and neither was perturbed by Dy^{3+}.

In contrast, sfGFP-2×dLBT exhibited a distinct behavior. Under 390 nm excitation, the biosensor emitted maximally at 510 nm and showed a substantial fluorescence increase in the presence of Dy^{3+} (Figure 3B). This signal was quenched by Ca^{2+}, but quenching was relieved upon the addition of 40 μM Dy^{3+}. Under 490 nm excitation, the emission maximum was red-shifted to 520 nm, but the metal-dependent effects were similar: Ca^{2+} (2 mM) quenched the fluorescence, whereas Dy^{3+} enhanced the overall signal (Figure 3C). Thus, the antithetical effects of Ca^{2+} and Dy^{3+} were consistently observed at both excitation/emission pairs (390/510 and 490/520), and the fold-change in Dy^{3+}-dependent fluorescence increased when the protein was pre-exposed to Ca^{2+} (Figure 3D).

To further characterize biosensor performance, we carried out a Dy^{3+} dose−response analysis using the optimal excitation−emission pairs identified above. For improved signal-to-noise ratio, 5 μM protein was used. Given the four metal-binding sites of 2×dLBT, we anticipated incomplete conformational activation below ∼20 μM Dy^{3+}. Consistent with this hypothesis, fluorescence increased proportionally with Dy^{3+} concentration at both excitation/emission settings. Although Ca^{2+} reduced the baseline fluorescence at low Dy^{3+} concentrations, similar fluorescence intensities were reached at Dy^{3+} > 500 μM, resulting in an enhanced fold-change in biosensor activation (Figure 3E,F).

The relatively high EC_{50} values observed for our biosensor can be explained by the stoichiometry of the sfGFP-2×dLBT construct, which contains four lanthanide-binding sites and therefore requires approximately a 4-fold molar excess of lanthanide to achieve full saturation and the associated conformational change. This is consistent with the response profiles observed at protein concentrations of 0.5 and 5 μM, which correspond to expected saturation points near 2 and 20 μM of lanthanides respectively, and limits of detection of ∼10 μM (Figure 2C) and ∼20 μM (Figure 3E,F), which translate to approximately 1.5−3 ppm of lanthanides in a solution. Many low-grade secondary resources such as acid mine tailings, phosphogypsum, e-waste leachates, and coal fly ash often contain total REEs in the range of 20−200 ppm.[17] Although not yet optimized for direct deployment in environmental matrices, the biosensor exhibits sensitivity within the relevant concentration range of lanthanides present in various secondary sources.

Our chimeric protein-based biosensor that responds to REEs can be genetically encoded and used to screen LBT variants that bind with a stronger affinity or react more efficiently to a specific REE, allowing development of a simple chemical reagent-free bioseparation process from samples that contain a mixture of several REEs such as phosphogypsum, acid mine drainage, and electronic waste leachates. In addition to mining and separation of electronic wastes, we envision that sfGFP-2×dLBT and its engineered derivatives would allow the determination of REE composition and the identification of REE-rich sources in an economic and rapid manner.

MATERIALS AND METHODS

Plasmid Construction

The expression plasmids for sLBT and 2×dLBT were constructed using the NEBuilder HiFi DNA Assembly Kit (New England Biolabs). The vector backbone, pET-28a(+) (Novagen), was linearized with NheI and *Bam*HI, and the DNA fragments encoding sLBT and 2×dLBT sequences were prepared with DNA synthesis (TWIST Bioscience). The assembled plasmids were transformed into NEB Turbo Competent *Escherichia coli* (New England Biolabs) according to the manufacturer's protocol. Transformed cells were grown overnight in lysogeny broth (LB) supplemented with 50 μg/mL kanamycin (LB-Kan_{50}) at 37 °C and 250 rpm for plasmid amplification. Plasmids were extracted using the Monarch Plasmid Miniprep Kit (New England Biolabs) following the manufacturer's instructions.

Protein Expression and Purification

For recombinant protein expression, plasmids encoding sfGFP-sLBT and sfGFP-2×dLBT were transformed into *E. coli* BL21 (DE3) cells (New England Biolabs). Transformed colonies were initially cultured overnight in 3 mL of LB-Kan_{50} at 37 °C and 250 rpm. The overnight culture was diluted to an initial OD_{600} of 0.1 in 200 mL of LB-Kan_{50} and incubated at 37 °C and 250 rpm until the OD_{600} reached ∼0.8. Protein expression was induced with 1 mM IPTG, and cells were further incubated at 30 °C for 5 h. Cells were harvested by centrifugation at 4000*g* for 15 min and resuspended in lysis buffer (buffer A: 300 mM NaCl, 50 mM K_2HPO_4, pH 7.2) containing 10 mM imidazole. Cells were lysed by sonication on ice in BugBuster MasterMix (Novagen) with EDTA-free protease inhibitor cocktail (Roche), clarified by centrifugation at 20,000*g* for 30 min at 4 °C, and the supernatant containing the soluble protein fraction was collected.

https://doi.org/10.1021/acsomega.5c10135
ACS Omega 2026, 11, 20235−20240

The proteins were purified using nickel affinity chromatography with a HisTrap High Performance column (Millipore Sigma) on a FPLC system. The column was equilibrated with Buffer A containing 10 mM imidazole, washed with Buffer A containing 20 mM imidazole, and eluted with Buffer A containing 300 mM imidazole. Following purification, the eluate was buffer exchanged into the assay buffer (50 mM HEPES, 150 mM NaCl, pH 7) using a desalting column.

The sfGFP-2×dLBT protein used for absorption−emission measurements and for evaluation at excitation−emission pairs of 390/510 and 490/520 nm was prepared as described above with additional purification steps. To prevent any unintended metal interactions, the 8 × His tag was removed by TEV protease digestion. The tag-free chimeric protein was then incubated with EDTA at an 8:1 molar ratio (EDTA/protein) at 25 °C for 10 min. Finally, ∼1 mL protein sample was dialyzed three times against 500 mL of assay buffer (50 mM HEPES, 150 mM NaCl, pH 7), resulting in a greater than 100-million-fold dilution of EDTA.

The GFP controls for the assays were also expressed in *E. coli*. 6 × His-tagged folding reporter GFP (FR-GFP) was purified using Ni-NTA affinity chromatography. The tagless superfolder GFP (sfGFP) was enriched from the cell lysate by briefly heating at 60 °C for 10 min, followed by centrifugation at 20,000*g* for 20 min to remove the aggregated bacterial proteins. The proteins were run on SDS-PAGE, and purity was evaluated using Image Lab software (Bio-Rad). The protein concentrations were measured using Abs_{280} on a nanodrop and corrected for percent purity based on densitometry.

Metal Ion Solution Preparation

Rare-earth element (REE) nitrate [lanthanum(III) nitrate hexahydrate (>99.9%), neodymium(III) nitrate hexahydrate (>99.9%), dysprosium(III) nitrate hexahydrate (>99.9%), terbium(III) nitrate hexahydrate (>99.9%)] and calcium chloride dihydrate (>99%) stock solutions (Sigma-Aldrich) were prepared at a concentration of 100 mM in Milli-Q water. For REE−protein binding assays, the stock solutions were serially diluted in 10-fold steps using the reaction buffer. The solutions of other non-REE metals were also made in Milli-Q water using nickel(II) chloride (98%), manganese(II) chloride tetrahydrate (>99%), copper(II) chloride dihydrate (>99%), aluminum potassium sulfate dodecahydrate (>98%), iron(II) sulfate heptahydrate (>99.9%), magnesium sulfate heptahydrate (>98%), and zinc sulfate heptahydrate (>99%) salts.

Metal Ion Binding Assay and Fluorescence Analysis

Metal-binding fluorescence assays were performed in black 96-well microplates to minimize signal cross-talk and background fluorescence. Each well contained 100 μL of purified protein diluted to a final concentration of 0.5, 5, or 10 μM in the assay buffer (50 mM HEPES, 150 mM NaCl, pH 7). REE solutions were added at 0.5−2 μL per well to achieve the desired final REE concentrations, which gave Ln^{3+}/LBT ratios of 100−4000 for sfGFP-sLBT and 5−1000 for 2×dLBT (considering four LBT sequences per 2×dLBT). For negative control wells, 1 μL of assay buffer was added in place of a metal solution. Plates were incubated at room temperature for 30 min with gentle shaking. Fluorescence measurements were recorded using a Synergy H4 Hybrid Plate Reader (BioTek) using settings for GFP fluorescence (excitation wavelength: 485 nm; emission wavelength: 528 nm). To ensure comparability across plates, fluorescence values were normalized as fold-changes relative to the corresponding negative controls (protein without any metal) on each plate.

Each well contained 100 μL of 0.5 μM sfGFP-2×dLBT and 2 mM Dy^{3+} with or without 2 mM Ca^{2+} and incubated at room temperature for 30 min with gentle shaking. The absorption (excitation) and emission spectra of Dy^{3+}-bound sfGFP-2×dLBT in the presence and absence of Ca^{2+} were measured on a Synergy H4 Hybrid Plate Reader (BioTek) over a range of 300−700 nm. All fluorescence values were normalized as fold-changes relative to the corresponding negative control.

■ ASSOCIATED CONTENT

Supporting Information

The Supporting Information is available free of charge at https://pubs.acs.org/doi/10.1021/acsomega.5c10135.

Additional figures for biosensor characterization, AlphaFold predicted structure; excitation/emission spectra (Figures S1−S7); and amino acid sequence of biosensors developed in the current work (Table S1) (PDF)

■ AUTHOR INFORMATION

Corresponding Author

Ramesh K. Jha − *Bioscience Division, Los Alamos National Laboratory, Los Alamos, New Mexico 87545, United States;* orcid.org/0000-0001-5904-3441; Email: rjha@lanl.gov

Authors

Jingyao Li − *Bioscience Division, Los Alamos National Laboratory, Los Alamos, New Mexico 87545, United States;* orcid.org/0000-0002-6834-4681

Sandra Oloketuyi − *Bioscience Division, Los Alamos National Laboratory, Los Alamos, New Mexico 87545, United States*

Li-Wei Hung − *Bioscience Division, Los Alamos National Laboratory, Los Alamos, New Mexico 87545, United States;* orcid.org/0000-0001-6690-8458

Nilusha Sudasinghe − *Chemistry Division, Los Alamos National Laboratory, Los Alamos, New Mexico 87545, United States*

Sang-Min Shin − *Bioscience Division, Los Alamos National Laboratory, Los Alamos, New Mexico 87545, United States;* orcid.org/0000-0002-5794-5510

Complete contact information is available at: https://pubs.acs.org/10.1021/acsomega.5c10135

Author Contributions

[§]J.L. and S.O. contributed equally. N.S., S.-M.S., and R.K.J. conceptualized the work. J.L. performed research. S.O. and L.-W.H. contributed to data analysis. N.S., S.-M.S., and R.K.J. acquired funding for the project. N.S., S.-M.S. and R.K.J. directed research. The manuscript was written through contributions from all authors. All authors have given approval to the final version of the manuscript.

Funding

Research presented in this article was supported by the Laboratory Directed Research and Development program of Los Alamos National Laboratory under project number 20240316ER. S.O. was supported by the Laboratory Directed Research and Development Director Fellowship program under the project number 20240862PRD2. This article is approved for Los Alamos Unlimited Release under LA-UR-25-29332.

Notes

The authors declare no competing financial interest.

■ ACKNOWLEDGMENTS

This work was supported by the U.S. Department of Energy through the Los Alamos National Laboratory. Los Alamos National Laboratory is operated by Triad National Security, LLC, for the National Nuclear Security Administration of U.S. Department of Energy (Contract No. 89233218CNA000001).

ABBREVIATIONS

CBP calmodulin-binding protein
GEFI genetically encoded fluorescence indicator
GFP green fluorescent protein
IPTG isopropyl-D-1-thiogalactopyranoside
LBT lanthanide-binding tag
PFAS per- and polyfluoroalkyl substances
sfGFP superfolder green fluorescent protein

REFERENCES

(1) Eliseeva, S. V.; Bünzli, J.- C. G. Lanthanide Luminescence for Functional Materials and Bio-Sciences. *Chem. Soc. Rev.* **2010**, *39* (1), 189−227.
(2) Weber, A. S.; Grady, A. M.; Koodali, R. T. Lanthanide Modified Semiconductor Photocatalysts. *Catal. Sci. Technol.* **2012**, *2* (4), 683−693.
(3) Mwewa, B.; Tadie, M.; Ndlovu, S.; Simate, G. S.; Matinde, E. Recovery of Rare Earth Elements from Acid Mine Drainage: A Review of the Extraction Methods. *J. Environ. Chem. Eng.* **2022**, *10* (3), 107704.
(4) Chen, Z.; Li, Z.; Chen, J.; Kallem, P.; Banat, F.; Qiu, H. Recent Advances in Selective Separation Technologies of Rare Earth Elements: A Review. *J. Environ. Chem. Eng.* **2022**, *10* (1), 107104.
(5) Franz, K. J.; Nitz, M.; Imperiali, B. Lanthanide-Binding Tags as Versatile Protein Coexpression Probes. *ChemBioChem* **2003**, *4* (4), 265−271.
(6) Sculimbrene, B. R.; Imperiali, B. Lanthanide-Binding Tags as Luminescent Probes for Studying Protein Interactions. *J. Am. Chem. Soc.* **2006**, *128* (22), 7346−7352.
(7) Cotruvo, J. A.; Featherston, E. R.; Mattocks, J. A.; Ho, J. V.; Laremore, T. N. Lanmodulin: A Highly Selective Lanthanide-Binding Protein from a Lanthanide-Utilizing Bacterium. *J. Am. Chem. Soc.* **2018**, *140* (44), 15056−15061.
(8) Mattocks, J. A.; Jung, J. J.; Lin, C.-Y.; Dong, Z.; Yennawar, N. H.; Featherston, E. R.; Kang-Yun, C. S.; Hamilton, T. A.; Park, D. M.; Boal, A. K.; Cotruvo, J. A. Enhanced Rare-Earth Separation with a Metal-Sensitive Lanmodulin Dimer. *Nature* **2023**, *618* (7963), 87−93.
(9) Park, D. M.; Reed, D. W.; Yung, M. C.; Eslamimanesh, A.; Lencka, M. M.; Anderko, A.; Fujita, Y.; Riman, R. E.; Navrotsky, A.; Jiao, Y. Bioadsorption of Rare Earth Elements through Cell Surface Display of Lanthanide Binding Tags. *Environ. Sci. Technol.* **2016**, *50* (5), 2735−2742.
(10) Pédelacq, J.-D.; Cabantous, S.; Tran, T.; Terwilliger, T. C.; Waldo, G. S. Engineering and Characterization of a Superfolder Green Fluorescent Protein. *Nat. Biotechnol.* **2006**, *24* (1), 79−88.
(11) Martin, L. J.; Hähnke, M. J.; Nitz, M.; Wöhnert, J.; Silvaggi, N. R.; Allen, K. N.; Schwalbe, H.; Imperiali, B. Double-Lanthanide-Binding Tags: Design, Photophysical Properties, and NMR Applications. *J. Am. Chem. Soc.* **2007**, *129* (22), 7106−7113.
(12) Mann, M. M.; Berger, B. W. A Genetically-Encoded Biosensor for Direct Detection of Perfluorooctanoic Acid. *Sci. Rep.* **2023**, *13* (1), 15186.
(13) Dana, H.; Sun, Y.; Mohar, B.; Hulse, B. K.; Kerlin, A. M.; Hasseman, J. P.; Tsegaye, G.; Tsang, A.; Wong, A.; Patel, R.; Macklin, J. J.; Chen, Y.; Konnerth, A.; Jayaraman, V.; Looger, L. L.; Schreiter, E. R.; Svoboda, K.; Kim, D. S. High-Performance Calcium Sensors for Imaging Activity in Neuronal Populations and Microcompartments. *Nat. Methods* **2019**, *16* (7), 649−657.
(14) Jones, E. M.; Su, Y.; Sander, C.; Justman, Q. A.; Springer, M.; Silver, P. A. LanTERN: A Fluorescent Sensor That Specifically Responds to Lanthanides. *ACS Synth. Biol.* **2024**, *13* (3), 958−962.
(15) Nitz, M.; Sherawat, M.; Franz, K. J.; Peisach, E.; Allen, K. N.; Imperiali, B. Structural Origin of the High Affinity of a Chemically Evolved Lanthanide-Binding Peptide. *Angew. Chem.* **2004**, *116* (28), 3768−3771.
(16) Jumper, J.; Evans, R.; Pritzel, A.; Green, T.; Figurnov, M.; Ronneberger, O.; Tunyasuvunakool, K.; Bates, R.; Žídek, A.; Potapenko, A.; Bridgland, A.; Meyer, C.; Kohl, S. A. A.; Ballard, A. J.; Cowie, A.; Romera-Paredes, B.; Nikolov, S.; Jain, R.; Adler, J.; Back, T.; Petersen, S.; Reiman, D.; Clancy, E.; Zielinski, M.; Steinegger, M.; Pacholska, M.; Berghammer, T.; Bodenstein, S.; Silver, D.; Vinyals, O.; Senior, A. W.; Kavukcuoglu, K.; Kohli, P.; Hassabis, D. Highly Accurate Protein Structure Prediction with AlphaFold. *Nature* **2021**, *596*, 583.
(17) Gaustad, G.; Williams, E.; Leader, A. Rare Earth Metals from Secondary Sources: Review of Potential Supply from Waste and Byproducts. *Resour., Conserv. Recycl.* **2021**, *167*, 105213.

https://doi.org/10.1021/acsomega.5c10135
ACS Omega 2026, 11, 20235−20240